Biogeosciences Discuss., 7, 5675–5718, 2010
www.biogeosciences-discuss.net/7/5675/2010/
doi:10.5194/bgd-7-5675-2010

Biogeosciences Discussions

Fluorescence and absorption properties of chromophoric dissolved organic matter (CDOM) in coastal surface waters of the Northwestern Mediterranean Sea (Bay of Marseilles, France)

J. Para[1,2], P. G. Coble[3], B. Charrière[1,2], M. Tedetti[1,2], C. Fontana[4,5], and R. Sempéré[1,2]

[1]Université de la Méditerranée, LMGEM, Centre d'Océanologie de Marseille, UMR 6117, Case 901, 13288 Marseille Cedex 9, France
[2]CNRS/INSU, UMR 6117, LMGEM, Case 901, 13288 Marseille Cedex 9, France
[3]College of Marine Science, University of South Florida, 140 7th Avenue, St. Petersburg, Florida 33701, USA
[4]Université de la Méditerranée, LOPB, Station Marine d'Endoume, Chemin Batterie des Lions, 13007 Marseille, France

[5]CNRS/INSU UMR 6535 – IRD (213), LOPB, Station Marine d'Endoume, Chemin Batterie des Lions, 13007 Marseille, France

Received: 28 June 2010 – Accepted: 6 July 2010 – Published: 22 July 2010

Correspondence to: R. Sempéré (sempere@univmed.fr)

BGD
7, 5675–5718, 2010

Abstract

Seawater samples were collected in surface waters (2 and 5 m depths) of the Bay of Marseilles (Northwestern Mediterranean Sea; 5° 17′ 30″ E, 43°14′ 30″ N) during one year from November 2007 to December 2008 and studied for total organic carbon (TOC) as well as chromophoric dissolved organic matter (CDOM) optical properties (absorbance and fluorescence). The annual mean value of surface CDOM absorption coefficient at 350 nm [$a_{CDOM}(350)$] was very low ($0.10 \pm 0.02\,m^{-1}$) with in comparison to values usually found in coastal waters, and no significant seasonal trend in $a_{CDOM}(350)$ could be determined. By contrast, the spectral slope of CDOM absorption (S_{CDOM}) was significantly higher ($0.023 \pm 0.003\,nm^{-1}$) in summer than in fall and winter periods ($0.017 \pm 0.002\,nm^{-1}$), reflecting either CDOM photobleaching or production in surface waters during stratified sunny periods. The CDOM fluorescence, assessed through excitation emission matrices (EEMs), was dominated by protein-like component (peak T; 1.30–21.94 QSU) and marine humic-like component (peak M; 0.55–5.82 QSU), while terrestrial humic-like fluorescence (peak C; 0.34–2.99 QSU) remained very low. This reflected a dominance of relatively fresh material from biological origin within the CDOM fluorescent pool. At the end of summer, surface CDOM fluorescence was very low and strongly blue shifted, reinforcing the hypothesis of CDOM photobleaching. Our results suggested that unusual Rhône River plume eastward intrusion events may reach Marseilles Bay within 2–3 days and induce local phytoplankton blooms and subsequent fluorescent CDOM production (peaks M and T) without adding terrestrial fluorescence signatures (peak C). Besides Rhône River plumes, mixing events of the entire water column injected humic (peaks C and M) CDOM from the bottom into the surface and thus appeared also as an important source of CDOM in surface waters of the Marseilles Bay. Therefore, the assessment of CDOM optical properties, within the hydrological context, pointed out several biotic (in situ biological production, biological production within Rhône River plumes) and abiotic (photobleaching, mixing) factors controlling CDOM transport, production and removal in this highly urbanized coastal area.

BGD

7, 5675–5718, 2010

1 Introduction

Dissolved organic matter (DOM) represents one of the largest bioreactive organic reservoirs at earth's surface (Hedges, 1992, 2002) and constitutes the main substrate for heterotrophic bacteria growth (Azam et al., 1983). The dominant source of DOM in the ocean is phytoplankton through release of organic compounds during bacterial and viral lysis, exudation, excretion and grazing (Coble et al., 1998; Nelson et al., 1998; Myklestad, 2000). Though the inputs of terrestrial DOM represent only 2–3% of the total oceanic DOM pool, river inputs may be important in coastal oceanic areas (Opsahl and Benner, 1997) by changing local bacterial carbon demand (Sempéré et al., 2000) and increasing light attenuation (Blough and Del Vecchio, 2002; Nelson and Siegel, 2002).

Chromophoric (or colored) dissolved organic matter (CDOM), which is the fraction of DOM that absorbs light over a broad range of ultraviolet (UV) and visible wavelengths, is essentially controlled by in situ biological production, terrestrial inputs (sources), photochemical degradation, microbial consumption (sinks), as well as deep ocean circulation (Siegel et al., 2002; Nelson et al., 2007; Coble, 2007). CDOM is the major factor controlling the attenuation of UV radiation in the ocean (Kirk, 1994) and is highly photoreactive and efficiently destroyed upon exposure to solar radiation (Mopper and Kieber, 2000, 2002).

In the 1990's, excitation emission matrix (EEM) spectroscopy became the standard tool for characterizing fluorescence properties of CDOM. Since the work of Coble et al. (1990), which highlighted that the fluorescence properties of the Black Sea CDOM came from two types of fluorophores (humic-like and protein-like). Protein-like fluorescence, considered as a proxy for labile DOM (Yamashita and Tanaoue, 2003), has been frequently reported (Mopper and Schultz, 1993; De Souza-Sierra et al., 1994; Determann et al., 1994, 1996; Coble 1996; Mayer et al., 1999). The identification/quantification of humic-like and protein-like fluorophores from EEMs has thus allowed determining the dynamics of DOM in relation to its biological reactivity.

BGD
7, 5675–5718, 2010

In addition, fluorescence indices have also been used to assess the origin and dynamics of fluorescent CDOM, especially in the coastal areas subjected to freshwater inputs. The humification index (HIX, Zsolnay et al., 1999) and the biological index (BIX, Huguet et al., 2009) have been used to determine the relative degree of humification and autotrophic productivity of fluorescent CDOM, respectively.

Freshwater inputs play a major role in the Mediterranean Sea, significantly enhancing primary productivity (Cruzado and Velasquez, 1990; Joux et al., 2009). The annual fluvial loading of TOC to the Mediterranean Sea comprises 0.08–0.3% of the standing stock of TOC in the whole Mediterranean Basin (Sempéré et al., 2000) which is much higher than the average reported for the World Ocean (Smith and Hollibaugh 1993). Since the damming of the Nile, the Rhône River became the major source of fresh water and terrigenous particles to the Mediterranean Basin (Margat, 1992). Its mean freshwater discharge is around 1700 $m^3 s^{-1}$, which represents 90% of the total freshwater input in the Gulf of Lion's continental shelf (Durrieu de Madron et al., 2003) and ~3–14% and 10–12% of the overall total organic and inorganic carbon (TOC and TIC) river inputs to the Mediterranean Sea (Sempéré et al., 2000). Remote sensing observations (Forget et al., 1990; Devenon et al., 1992; Broche et al., 1998) and modeling studies (Estournel et al., 2001; Arnoux-Chiavassa et al., 2003; Reffray et al., 2004) showed the predominant westward direction of the Rhône River plume with an extent and a thickness that depend on its discharge, the meteorological conditions and the surrounding circulation, particularly the Northern Current. A less common orientation of the Rhône River plume, towards the east as far as 40 km from the Rhône River mouth and offshore of Marseilles Bay, has been recently documented by using the acoustic Doppler current profiler (ADCP) measurements (Gatti et al., 2006).

Despite its relative significant role in the Mediterranean carbon cycle, there are only a few studies showing CDOM originating either directly from the Rhône River or as by-products of primary production in coastal areas or more generally in the Northwestern Mediterranean Sea (Ferrari et al., 2000; Babin et al., 2003; Vignudelli et al., 2004). Moreover, with an annual average of total solar radiation of 162 $W m^2$ (Ruiz et al.,

BGD
7, 5675–5718, 2010

2008), the Western Mediterranean Basin is characterized by relatively high solar radiation levels due to its weak cloud cover (Vasilkov et al., 2001; Seckmeyer et al., 2008; Cristofanelli and Bonasoni, 2009; The MERMEX group, 2010). High insolation coupled to a strong penetration of UV and visible radiation (Tedetti and Sempéré, 2006 and references therein; Joux et al., 2009) could impact CDOM content as well as primary productivity in the surface waters.

Here we report for the first time CDOM absorbance and fluorescence data from a one-year time series in the Bay of Marseilles. This study aims to better understand coastal surface CDOM distribution and dynamic of the Mediterranean Sea. Origins as well as seasonal variation of CDOM are discussed considering the potential Rhône River plume influence.

2 Materials and methods

2.1 Study site and sample collection

From November 2007 to December 2008, surface seawater samples (2 and 5 m depths) were collected monthly close to solar noon using Niskin bottles equipped with Teflon-O-ring and silicon tubes. Surface irradiance ($E_s(\lambda)$ in $\mu W\,cm^{-2}$) measurements in the UV (305, 325, 340, 380 nm) spectral domain were also performed using OCR-504 downward irradiance sensors on the ship's deck on board the R/V Antedon II at the observation station of the Oceanology Center of Marseilles: SOFCOM. This coastal station is located 5 km off Marseilles in the Northwestern Mediterranean Sea (Fig. 1) and is one of the French Service d'Observation en Milieu LITtoral (SOMLIT, http://www.domino.u-bordeaux.fr/somlit_national/) coastal stations, which have been regularly sampled (twice a month) for 13 years. During this study period, water samples were also collected at 2 m depth in the Rhône River at Arles station, and from 2 and 5 m depths at two stations in the Rhône River estuary during the CHACCRA-plume cruise (May 2008) (Fig. 1).

BGD
7, 5675–5718, 2010

For total organic carbon (TOC) determination, samples were directly transferred from the Niskin bottle into precombusted (6 h at 450 °C) ampoules, immediately acidified with 85% of H_3PO_4 (final pH~2) and flame sealed without filtration. For CDOM optical properties determination (absorbance and fluorescence), samples were transferred from Niskin bottles into 10% HCl washed and precombusted (6 h at 450 °C) glass bottles and stored in the dark. Samples were brought back to the laboratory, filtered in dim light through precombusted 0.7 µm GF/F filters, which had been pre-rinsed with Milli-Q water and sample, and then through 0.2 µm Nuclepore polycarbonate filters, presoaked in 10% HCl solution and rinsed with Milli-Q water and with sample according to the SeaWiFS protocols (Mueller and Austin, 1995). Filtered samples were kept in the dark at room temperature (24 h maximum) until absorbance and fluorescence analyses. During the study period, in situ hydrological context was determined at least twice a month by the Service d'Observation of the Oceanology Center of Marseilles by using a SeaBird Electronics 19*plus* conductivity temperature depth (CTD) profiler. In addition, from February 2008 onwards, the hydrological data set was completed with a SeaBird Electronics 19*plus* CTD equipped with chlorophyll-*a* (Chl-*a*) fluorometer (WET Labs Inc.) deployed during our sampling. Sampling dates and parameters measured are reported in Table 1.

2.2 CDOM optical properties

2.2.1 Absorbance measurements

Absorbance of CDOM was measured throughout the UV and visible spectral domains (280–700 nm) using the multiple pathlength, liquid core waveguide system Ultrapath (MPLCW, WPI Inc.). Absorbance spectra of SOFCOM and Rhône plume samples (marine samples) were measured with reference to a filtered salt solution prepared with Milli-Q water and precombusted NaCl (Sigma) reproducing the refractive index of samples to minimize baseline offsets in absorption spectra (D'Sa et al., 1999), while filtered Milli-Q water was used as the blank for Rhône River samples (freshwater samples).

BGD
7, 5675–5718, 2010

Reference salt solution and samples were brought to room temperature before analysis. Between each sample, the sample cell was flushed with successively diluted detergent (Cleaning solution concentrate, WPI Inc.), high reagent grade MeOH, 2 M HCl and Milli-Q water. Cleanliness of the sample cell was checked by comparing with a reference value for the transmittance of the reference salt solution. Trapped microbubbles were minimized by using a peristaltic pump to draw the sample into the sample cell. The spectral absorption coefficients, $a_{CDOM}(\lambda)$ (m^{-1}) were obtained using the following relationship, $a_{CDOM}(\lambda)=2.303\,A(\lambda)/L$, where $A(\lambda)$ is the absorbance at wavelength λ (dimensionless) and L is the pathlength in meters. Value of spectral slope of CDOM absorption (S_{CDOM}) has most often been determined using an exponential regression (Jerlov, 1968; Bricaud et al., 1981) but non-linear regression fitting provides a better estimate of S_{CDOM}, by weighting regions of higher CDOM absorption (Del Vecchio and Blough, 2004). Here, S_{CDOM} was determined by applying a non-linear fit of log-linearized absorption data in the spectral range 350–500 nm (R^2>0.99). S_{CDOM} provides information concerning CDOM origin (terrestrial *versus* marine), with generally lower slopes in fresh and coastal waters than in the open ocean due to the presence of marine humics and new biological CDOM (Ferrari et al., 2000; Blough and Del Vecchio, 2002). Additionally, higher S_{CDOM} have been reported for photobleached CDOM (Vodacek et al., 1997).

2.2.2 Fluorescence measurements

For fluorescence measurements, samples were transferred into a 1 cm pathlength far UV silica quartz cuvette (170–2600 nm; LEADER LAB), thermostated at 20 °C, and analyzed with a Hitachi (Japan) Model F-7000 spectrofluorometer. Instrument settings, measurement procedures and spectral correction procedures are fully described in Tedetti et al. (2010). Briefly, the correction of spectra for instrumental response was conducted according to the procedure recommended by Hitachi (Hitachi F-7000 Instruction Manual). First, the Ex instrumental response was obtained by using

BGD
7, 5675–5718, 2010

Rhodamine B as standard and a single-side frosted red filter in Ex scan mode. Then, the Em side calibration was done with a diffuser in synchronous scan mode. The Ex and Em spectra obtained over the range 200–600 nm were applied internally by the instrument to correct subsequent spectra. EEMs were generated over Ex wavelengths between 200 and 550 nm in 5 nm intervals and Em wavelengths between 280 and 600 nm in 2 nm intervals, with 5 nm bandwidths (FWHMs) on both Ex and Em sides and a scan speed of 2400 nm min^{-1}. Milli-Q water as well as solutions of quinine sulphate (Fluka) in 0.05 M H_2SO_4 (1–10 ppb) were run with each set of samples. Before being processed, all the data (blanks, standards, samples) were normalised to the intensity of the water Raman scatter peak at Ex/Em: 275/303 nm (5 nm bandwidths), used as an internal standard (Coble et al., 1993; Coble, 1996; Belzile et al., 2006), which varied by less than 4% over the study period. Samples were then corrected for the corresponding blanks and converted into quinine sulphate units (QSU). EEM data processing and contour plots were conducted with MATLAB 7.1.

Besides the identification of common fluorophores by the traditional "peak picking" technique (examination of Ex and Em spectra), we determined two indices: the humification index (HIX) and the biological index (BIX). HIX was introduced on the basis of the position of the emission spectra in order to estimate the degree of maturation of DOM in soil (Zsolnay et al., 1999). It is the ratio (H/L) of two areas of emission spectrum from excitation at 254 nm (here 255 nm). These two areas are calculated between 300 and 345 nm (here 346 nm) for *L* and between 435 (here 434 nm) and 480 nm for *H*. In natural aquatic ecosystem (Gironde and Seine estuaries and Mediterranean Sea), high values of HIX (10–16) illustrated the presence of strongly humic organic material (terrestrial origin), whereas low values (<4) represent authochtonous organic material (Huguet et al., 2009). BIX allows the determination of the presence of the marine humic-like peak (peak M), which reflects autochthonous biological activity (Huguet et al., 2009). It is calculated at Ex=310 nm (here 300 nm), by dividing the fluorescence intensity at Em=380 nm (maximum intensity of M, here 390 nm) by the fluorescence intensity at Em=430 nm (here 440 nm), which corresponds to the maximum of peak

BGD
7, 5675–5718, 2010

C. High values of BIX (>1) correspond to a biological origin and lowest values (<1) illustrate low abundance of organic matter of biological origin (Huguet et al., 2009).

2.3 TOC analysis

The Shimadzu instrument used in this study is the commercially available model TOC-5000 Total Carbon Analyzer with a quartz combustion column filled with 1.2% Pt on silica pillows. Several aspects of our modified unit have been previously described (Sohrin and Sempéré, 2005). The accuracy and the system blank of our instrument were determined by the analysis of the reference material (D. Hansell, Rosenstiel School of Marine and Atmospheric Science, Miami, USA) including Deep Atlantic Water (DAW) and low carbon water (LCW) reference standards. The average DOC concentrations in the DAW and in the LCW reference standards were $45 \pm 2\,\mu M\,C$, n=24 and $10 \pm 3\,\mu M\,C$, n=24, respectively. Carbon levels in the LCW ampoules were similar to and often higher than the Milli-Q water produced in our laboratory. The nominal analytical precision of the analysis procedure was within 2%.

2.4 Remotely sensed data

Remotely sensed images of SST and Chl-*a* concentration (Fig. 2) were obtained by applying, respectively the long-wave SST algorithm and the OC5 coastal-oriented optical algorithm (Gohin et al., 2002, 2005) to water leaving irradiances derived from the Moderate Resolution Imaging Spectroradiometer (MODIS) sensor. Accuracy of the OC5 algorithm applied to the Rhône River plume region has been estimated to be 40% absolute percentage of difference by comparing 332 in situ and co-localized remotely sensed values of Chl-*a* concentrations using the Sea-viewing Wide Field of View Sensor (SeaWiFS) (Fontana et al., 2009).

BGD
7, 5675–5718, 2010

3 Results

3.1 Hydrological context and trophic status

During winter and fall periods, the action of winds mixed entirely the water column of Marseilles Bay (60 m depth). The general trend observed from the surface to the bottom during this stormy period was a salinity close to 38.1–38.2 and a temperature decrease from 18 to 15 °C in fall and from 15 to 13 °C in winter (Fig. 2). These are the typical values recorded for the Northwestern Mediterranean Sea (Brasseur et al., 1996). At the beginning of spring, the entire water column was still well mixed and exhibited a temperature and a salinity corresponding to those observed during winter (Fig. 2). During May, water began warming (16–17 °C) causing the formation of a thermocline around 40 m depth. Early in May, an intrusion of a less salty water mass (37–37.8) was observed in the upper 10 m. The low salinity surface water mass, perhaps coupled with physical forcing, seems to have also impacted the salinity signature of the deepest water because the salinity of the latter was <38 down to 45 m, whereas the salinity value of deeper Mediterranean water masses are usually close to 38.3 (Brasseur et al., 1996). At the end of June, another important surface intrusion of low salinity water occurred with a salinity ranging from 37.3 to 37.8 and a temperature ranging from 21.5 to 18 °C between 1 and 30 m depth, respectively. As for the previous low salinity intrusion, this one also appeared to influence the salinity signature of deeper water masses.

These two surface intrusions of low salinity water were also identified by remotely sensed pictures of SST and Chl-*a* concentration on 7 May 2008 (nearest date available corresponding to the sampling date 6 May 2008) on 23 June 2008 (sampling date) and were shown on Fig. 2 (insets a and b). These remotely sensed pictures plus those available encompassing sampling dates (not shown) illustrate clearly that surface inputs of freshwater observed on 6 May 2008 and on 23 June 2008 in Bay of Marseilles came from the eastward extent of the Rhône River plume. In addition, they allow us to estimate to 2–3 days minimum, the spreading time of Rhône River plume to reach

BGD
7, 5675–5718, 2010

surface waters of Bay of Marseilles located at about 40 km eastward which is in agreement with the scale time observed by Fontana et al. (2010).

In July, 3 consecutive days of wind from north (Mistral wind) mixed the water column, removing all signs of the Rhône River plume and resulting in a cooling (14–15 °C) coupled to an increase of salinity (38.1) of surface waters (Fig. 2). Sea surface temperature dropped to 16.5 °C at 1 m depth, which is a specific feature of the Bay of Marseilles during stratification period under Mistral wind influence. The last part of summer (August) was more common with the reformation of the thermocline around 15–20 m depths separating warm (18–23 °C) and salty (38.2) surface waters from cold deep waters (14–18 °C) of slightly lower salinity (38). At the end of summer (23 September 2008), a warm (21–22 °C) high salinity (>38.4) water mass was observed from a depth of 20 m to the surface which was replaced on 14 October 2008 by a shallower low salinity water mass (37.6) in the upper 3 m due to intense rains. Other slightly less saline water masses in surface were observed at the end of November 2007 and early in December 2008 but during these windy periods, surface low salinity water masses were attenuated and disappeared rapidly due to the mixing (Fig. 2).

In early May and at the end of June 2008, the influence of the eastward extent of the Rhône River could have increased nitrates concentrations within the plume along a gradient of salinity (10–36) from 90 to 15 µM (Pujo-Pay et al., 2006) as well as others nutrients to lesser extent. Primary production in the Bay of Marseilles was enhanced with a value of Chl-*a* concentration >1 µg l^{-1} (Table 2, Fig. 2 insets), while without the influence of the Rhône River plume Chl-*a* concentration remained <1 µg l^{-1}. At SOFCOM station, TOC concentrations at both depths studied were similar and were also comparable to DOC concentrations previously reported in open waters of Mediterranean Sea (Doval et al., 1999; Dafner et al., 2001; Santinelli et al., 2002; Sempéré et al., 2002; Seritti et al., 2003), with a stable annual mean of 67 ± 7 µM C at 2 m and 63 ± 6 µM C at 5 m. Thus, despite some episodic influence of the Rhône River plume, this coastal area exhibited features including Chl-*a* concentration <1 µg l^{-1} and TOC concentration~DOC concentration, that are usually encountered offshore. It is

BGD
7, 5675–5718, 2010

important to notice this coastal oligotrophic area is subjected to a strong UV surface irradiance particularly in spring and summer periods for UVB (305 nm) radiation with surface irradiance (Es) values as high as 4.64 $\mu W\,cm^{-2}\,nm^{-1}$ for UVB (305 nm) in summer time (Table 2) around solar noon. Indeed, with the exception of sampling dates that were cloudy, we observed around 10 fold more UVB (305 nm) and 2–3 fold more UVA (325, 340 and 380 nm) radiation in summer and spring compared to fall and winter periods.

3.2 CDOM absorbance

The a_{CDOM} at 350 nm was chosen for describing changes in CDOM quantity, and S_{CDOM} to differentiate CDOM quality (Table 2). At the SOFCOM station during the study period (November 2007 to December 2008), the annual mean values of $a_{CDOM}(350)$ at 2 and 5 m depths were comparable and very low ($0.10 \pm 0.02\,m^{-1}$) with regard to the entire range of the $a_{CDOM}(350)$ found in the literature for diverse oceanic waters (i.e. 0.046–29.9 m^{-1}) and thus were more similar to those found offshore. The $a_{CDOM}(350)$ maximum value of $0.13\,m^{-1}$ at 2 and 5 m was observed under Rhône River plume influence (5 June 2008) and during the fall mixing period (25 November 2008), right after 12 consecutive days of Mistral wind that initiated a strong mixing of the entire water column. By contrast, $a_{CDOM}(350)$ minimum value at 2 m ($0.07\,m^{-1}$) and 5 m ($0.06\,m^{-1}$) occurred at the end of summer time (23 September 2008) (Table 2), when the highest salinity (>38.4) and high temperature (22 °C) water was observed (Fig. 2). Since no significant seasonal trend of $a_{CDOM}(350)$ appeared during this period, our results suggest that external influences such as Rhône River plume intrusion and deep mixing events control CDOM surface content and variability in Marseilles coastal area.

The annual mean of S_{CDOM} determined during this study was $0.019 \pm 0.003\,nm^{-1}$ at both depths and was in the range previously established by Ferrari (2000) for October 1997 at the surface in vicinity of Rhône River mouth ($0.018 \pm 0.003\,nm^{-1}$) and for surface blue waters of the Gulf of Lions ($0.017 \pm 0.003\,nm^{-1}$). S_{CDOM} extreme values

BGD
7, 5675–5718, 2010

(2 and 5 m) ranged from 0.014 nm^{-1} on 25 November 2008 to 0.026 nm^{-1} on 23 June 2008 (Table 2). Seasonal means of S_{CDOM} were the lowest and comparable during fall and winter periods (S_{CDOM} at 2 and 5 m=0.017 ± 0.002 nm^{-1}) while during summer time S_{CDOM} were significantly higher (U-Test, p<5%, n=3–4) with seasonal mean value reaching 0.023 ± 0.003 nm^{-1} and 0.024 ± 0.002 nm^{-1} at 2 and 5 m depths, respectively. Spring means of S_{CDOM} were in the middle of the range with 0.020 ± 0.002 nm^{-1} and 0.019 ± 0.003 nm^{-1} at 2 and 5 m depths, respectively.

The significant inverse relationship between salinity and $a_{CDOM}(350)$ for the shallowest depth studied (2 m) (Fig. 3) indicates a conservative behavior for surface CDOM absorbance. The CDOM absorption mixing line established using SOFCOM data at 2 m depth with salinity <38 (on 6 May 2008, 9 June 2008, 23 June 2008, 10 July 2008) plus two data points acquired close to the Rhône estuary in the Rhône River plume at 2 m depth in May 2008 has an intercept of 1.20 m^{-1}, which is in the range of that calculated for the Rhône River end member at Arles station (1.65 ± 0.53 m^{-1}) during the same period (May–July 2008; Table 2). Moreover, when data from the Rhône River plume are excluded and all the SOFCOM data at both 2 and 5 m depths were used except the extreme values (23 September 2008 and 25 November 2008), another significant inverse relation was observed (p<1%, n=11 at 2 m and n=12 at 5 m), with $a_{CDOM}(350)$=−0.032 salinity+1.33), which is comparable to the previous calculation. Points above the mixing line in Fig. 3 represent a net production of CDOM. The most important net production of CDOM was associated with low TOC concentration values (55–56 µMC) and with the lowest S_{CDOM} (0.014 nm^{-1}) values and occurred at both depths during a strong mixing event (25 November 2008). By contrast, the two points that fall far below the mixing line also present the highest salinities (38.4), high temperature (22 °C), high S_{CDOM} values (0.021–0.023 nm^{-1}), as well as moderately high E_s [1.13 µW cm^{-2} nm^{-1} for UVB (305 nm)] and were collected at the end of summer time (23 September 2008).

BGD
7, 5675–5718, 2010

3.3 CDOM fluorescence

All the fluorescence peaks observed during the fluorescence study period (June 2008–December 2008) can be summarized from the 3 samples collected on 23 June 2008, 23 September 2008 and 25 November 2008. EEMs for these samples are presented in Figs. 4 and 5 for 2 and 5 m depths, respectively, while peaks intensities for all samples are recapitulated in Table 3. During the period studied, peak T (tryptophan-like, Ex/Em=225/340 nm and 275/340 nm) was the major fluorophore present (6.45 ± 8.25 QSU at 2 m depth and 1.94 ± 0.93 QSU at 5 m depth), followed by peak M (UVA marine humic-like, Ex/Em=290–310/370–410 nm) with a mean value of 2.38 ± 2.15 QSU at 2 m depth and 1.74 ± 1.65 QSU at 5 m depth, and peak C (UVA humic-like Ex/Em=320–360/420–460 nm) which was the least intense (1.10 ± 0.99 QSU at 2 m depth and 0.93 ± 0.95 QSU at 5 m depth). Peak B (tyrosine-like, Ex/Em=225/305 nm and 275/305 nm) was found only on 23 June 2008. The most striking feature about all EEMs is the lack of peak A (UVC humic-like, Ex/Em=260/400–460 nm).

Maximum fluorescence intensities of peaks C, M and T (Table 3) at both depths occurred on 25 November 2008, during a strong mixing event enhanced by 12 consecutive days of Mistral wind and during a Rhône River plume extent event observed on 23 June 2008. For all other samples, all peak intensities were stable and low, especially in summer as observed on 10 July 2008 (despite the minor mixing event due to 3 consecutive days of Mistral wind) and 23 September 2008 (Table 3). The sample from 23 September 2008 showed a strong fluorescence signal in short Ex/Em wavelengths at both depths and possibly a slight signal of peak T as well (Figs. 4 and 5). This kind of signal at short wavelengths has been previously observed in strongly photobleached samples (P. Coble, unpublished data).

In contrast to the significant relationship between surface $a_{CDOM}(350)$ and salinity, there was only a weak inverse relationship (p<5%, n=6, data not shown) between fluorescence of peaks C and M (Table 3) and salinity at 5 m depth and excluding the

BGD
7, 5675–5718, 2010

maximum values (25 November 2008). This result indicates that fluorescent CDOM character in the surface is (1) mainly driven by other processes than water mixing and (2) less conservative than is absorbant homologue.

Additional information concerning the quality (purity) of peaks M and C can be illustrated through their normalized emission spectra (Fig. 6) for the 3 same samples (23 June 2008, 23 September 2008 and 25 November 2008) shown in Figs. 4 and 5. Panels a and b show emission at the wavelength of maximum excitation for peak M (300 nm). The purest M peaks were observed on 25 November 2008 sample at both depths, evidenced by the narrower peak width (dashed line). The samples collected on 23 June 2008 (dotted line) and 23 September 2008 (dashed-dotted line) have a broader emission maximum with shoulder around 450 nm. Moreover, during Rhône River plume intrusion event (23 June 2008), an overlapping of the peak M by the peak T could be observed at the emission band 350–370 nm at 2 m depth. Panels c and d show emission at the wavelength of maximum excitation for peak C (350 nm). Again, the sample collected on 25 November 2008 shows a narrower peak width at both depths, whereas the samples collected on 23 June 2008 and 23 September 2008 have a broader emission maximum with shoulder around 470 nm. Taken together, the spectra indicate that the CDOM collected in the November 2008 sample was the purest material. This is consistent with recent deep mixing conditions as well as low TOC concentration values observed at this date.

4 Discussion

4.1 Evidence for a biological origin of CDOM

Our results indicate that, despite the low and quite stable values of $a_{CDOM}(350)$ determined in surface waters of the Bay of Marseilles, the significant inverse linear relationship observed at both depths between $a_{CDOM}(350)$ and salinity illustrated a conservative behavior of surface CDOM in this area. This represents the first report of

BGD
7, 5675–5718, 2010

the potential biogeochemical influence of the Rhône River plume in this oligotrophic coastal area. Such a strong significant inverse relationship between salinity and fluorescent/absorbant CDOM is typically observed in coastal areas subjected to high river inputs (Blough et al., 1993; Green and Blough, 1994; Nelson and Guarda, 1995; Højerslev et al., 1996; Nieke et al., 1997; Vodacek et al., 1997; Seritti et al., 1998; Del Castillo et al., 2000; Ferrari, 2000; Stedmon et al., 2000).

By contrast, the lack of correlation between salinity and fluorescence intensities of peaks C and M at 2 m depth (excluding the maximum values, 25 November 2008) and the only weakly significant correlation observed for 5 m depth samples suggest that the Rhône River plume is not a dominant source of fluorescent CDOM in Marseilles Bay. Fluorescent CDOM content in surface waters is likely driven by others processes such as in situ production or photo-oxidation rather than water mixing as already hypothesized by Vignudelli et al. (2004) for coastal waters of the Northern Tyrrhenian Sea (Italy). The first of these processes is penetration of UV solar radiation inducing photobleaching, which is more destructive of fluorescence than of absorbance (Moran et al., 2000; Nieto-Cid et al., 2006). This phenomenon is likely observed during water stratification, especially during spring and summer periods when UV irradiance is high (Table 2). Therefore, it is very likely that samples collected at the end of summer period (23 September 2008), were strongly photobleached of all fluorescence in the M and C regions (Figs. 4 and 5). This assumption would be consistent with high S_{CDOM} coupled to low $a_{CDOM}(350)$ values that fell beneath the mixing line in Fig. 3, and suggest a net loss of CDOM at this time. In situ production is another process that may modify CDOM fluorescence character. Indeed, phytoplankton production (Romera-Castillo et al., 2010), zooplankton grazing (Coble et al., 1998) and bacterial activity (Stedmon and Markager, 2005) may induce production of fluorescent CDOM through production of by-products, especially peaks B, T, and M. Primary production and bacterial activity promoted by the Rhône River plume intrusion event rich in nutrients (Chl-*a* concentration $>1\,\mu g\,l^{-1}$; on 6 May 2008 and 23 June 2008) may have produced fluorescent CDOM. Finally, the strong mixing observed on 25 November 2008 sample could have

BGD
7, 5675–5718, 2010

injected CDOM from the bottom to the surface as well as nutrients and thus explain an increase of surface CDOM concentrations (Coble et al., 1998; Nelson et al., 2004, Nieto-Cid et al., 2006). Samples collected on these three dates all fall above the mixing line in Fig. 3 and thus are indicative of a net production of CDOM.

Surface CDOM content in the Bay of Marseilles results, therefore, from some combination of processes which differentially affect its fluorescence and absorbance properties. In any case, our results strongly suggest that CDOM properties in this area might be modified by autochthonous production induced by the Rhône River plume intrusion and not primarily from the Rhône River itself.

In Marseilles Bay, during the one year survey, surface CDOM exhibited very low and stable $a_{CDOM}(\lambda)$ and high variability of S_{CDOM}, highest values being observed during summer time. Generally such signals as well as low surface TOC concentration and Chl-*a* concentration are observed offshore (Blough and Del Vecchio, 2002) or in an oligotrophic coastal area not influenced by river inputs. High S_{CDOM} could reflect either CDOM photobleaching if $a_{CDOM}(\lambda)$ is low as observed on 23 September 2008 or fresh biological CDOM production in surface waters if $a_{CDOM}(\lambda)$ is high as observed on 23 June 2008. By contrast, low S_{CDOM} with high $a_{CDOM}(\lambda)$ as observed on 25 November 2008 suggest the presence of humic CDOM in surface that could be the consequence of the strong mixing of deep water that was reported at this period.

Concerning CDOM fluorescence properties, our study showed the dominance of autochthonous compounds (peaks T and M) and extremely low values of terrestrial humic substances (peak C) within surface fluorescent CDOM pool. Fluorescence intensity of peak T observed on all dates (except on 23 June 2008 and 25 November 2008) at 2 and 5 m depths (Table 3) was in accordance to that reported in surface Ise Bay in the Pacific coastal area (Yamashita and Tanoue, 2003). Interestingly, during Rhône River plume intrusion and mixing events in Marseilles Bay, fluorescence intensity of peak T was one order of magnitude higher at 2 m depth (Table 3). The origins of peaks T and M have been attributed to planktonic activity (Determann et al., 1998; Myklestad, 2000; Nieto-Cid et al., 2006; Romera-Castillo et al., 2010) while the origin of peak C is

BGD
7, 5675–5718, 2010

known to be terrestrial and thus came from freshwater inputs (Sierra et al., 1997; 2005; Komada et al., 2002) and also from upward mixing of deeper ocean water (Coble et al., 1998). Mayer et al. (1999) in two Maine estuaries (Atlantic Ocean) observed that seawater samples tended to show higher tyrosine (peak B) while upstream samples were richer in tryptophan (peak T). Thus, these observations, in accordance with our results concerning the peak T, could provide an explanation for the lack of peak B (except on 23 June 2008) observed in the Bay of Marseilles. Samples in this study exhibiting high peak T and low peak B, may indicate fresher material recently produced (Mayer et al., 1999).

To reinforce the hypothesis of the biological source of surface fluorescent CDOM in Marseilles Bay, three fluorescence indices were also calculated including HIX, BIX and M/C peaks ratio (Table 4). Our results showed low and variable values of HIX and high constant values of BIX at SOFCOM station, suggesting a predominantly autochthonous origin of DOM and the presence of organic matter freshly released in surface waters. The lack of terrestrial signature of CDOM is surprising particularly during Rhône River plume intrusion, easily detected on 23 June 2008 from remote sensing observations. At this date, the lowest HIX value was observed at 2 m depth (0.42) while it was around 3 fold more important at 5 m depth (1.22). The efficiency of photo-oxidation process in surface layer could explain such different HIX values between 2 and 5 m depths. Indeed, a significant proportion, as high as 96%, of CDOM from freshwater (i.e. humic material) might be destroyed during long term exposure to solar radiation (Vähätalo and Wetzel, 2004). Grzybowski (2000) estimated riverine CDOM to be 10 fold more sensitive than coastal CDOM to photobleaching, with the effects of this process being detectable after only 6 h of exposure under natural sunlight. During the eastward spreading of the buoyant Rhône River plume on surface marine waters, an important part of the terrestrial CDOM pool could be removed, as well as a part of the autochthonous CDOM freshly produced, if any, due to photobleaching (Vodacek et al., 1997; Del Castillo et al., 1999). Thus, photobleaching could explain the lack of terrestrial fluorescence signature in this coastal area, where the spreading

BGD
7, 5675–5718, 2010

time of Rhône River plume to reach surface waters of Marseilles Bay was estimated at 2–3 days minimum.

High and constant BIX values at both depths illustrated the omnipresence of the peak M, characterizing an autochthonous biological activity which was slightly more important at 2 m than 5 m depth (except on 10 July 2008 during a mixing event), particularly under Rhône River plume influence (23 June 2008). The competing process of photobleaching probably hid a part of this biological activity especially in the surface waters. The highest BIX values at 2 m depth determined on 23 June 2008 and 25 November 2008 corresponded, respectively to an important Rhône River plume intrusion containing freshly produced CDOM and to a strong water column mixing that may injected humic CDOM in surface waters. The M/C ratio reflects the relative amount of new (marine) to old (terrestrial) CDOM. On 23 June 2008, higher values found at 2 m relative to 5 m depth reinforces either the observation that biological activity is likely more developed at 2 m and the power of UV radiation to bleach terrestrial CDOM.

The discrimination between marine phytoplankton and bacteria as the predominant biological source of peak T can be assessed through spectral analyses of this peak according to the criteria of Determann et al. (1998). Normalized emission spectra at Ex=230 nm at both depths (Fig. 7, panels b and d) exhibited peaks position in the 325–345 nm range while the one of free dissolved L-tryptophan used as standard was around 360 nm, in agreement with the findings of Determann et al. (1998). A weak second band at 300 nm, specific to phytoplankton species, was only observed for samples from 23 June 2008 (black dotted line) and 23 September 2008 (black dashed-dotted line) and was more pronounced at 5 m than at 2 m. In normalized excitation spectra at Em=340 nm (Fig. 7, panels a and c), the main absorption band in the 220–230 nm range was clearly red shifted around the range 230–235 nm on 9 June 2008 at both depths and on 10 July 2008 at 5 m depth, as observed by Determann et al. (1998) with bacteria cultures. Moreover, at these dates and depths another absorption band (specific to bacteria) in the range 275–280 nm was observed while at the other dates a signal more or less constant was observed. Therefore, such results illustrate clearly

BGD
7, 5675–5718, 2010

a dominant phytoplankton origin for tryptophan at both depths on 23 June 2008 and 23 September 2008 while tryptophan had a dominant bacterial origin on 9 June 2008 at both depths and on 10 July 2008 at 5 m depth. Establishing the predominant biological origin for the other dates studied regarding emission and excitation spectra of tryptophan results is not straightforward, possibly due to an equal contribution of phytoplankton and bacteria origin to the tryptophan content. Interestingly the results of this discrimination were logical regarding the hydrological context. Indeed, dominant phytoplankton origin of tryptophan took place during bloom periods enhanced by nutrients inputs through an intrusion of the Rhône River plume (23 June 2008) and or through a mixing (23 September 2008), whereas dominant bacteria origin of tryptophan took place (9 June 2008 and 10 July 2008) after or during bloom events.

4.2 Seasonal evolution of surface CDOM

The results taken as a whole allow seasonal features of the surface CDOM content to be established for the Bay of Marseilles. In spring and summer time, when the water column becomes stratified, freshwater intrusions of the Rhône River plume were easily identifiable by lowered salinities (Fig. 2). The high nutrient content of this buoyant plume enhanced marine primary production in surroundings surface marine waters (Cruzado and Velasquez, 1990; Pujo-Pay et al., 2006; Joux et al., 2009) (Fig. 8). This would be consistent with our observations on 6 May 2008 and 23 June 2008. The time scale of its transport to the Bay of Marseilles under solar radiation certainly play a major role in the state of development of primary production associated with bacteria communities and also in the terrestrial CDOM content and properties (Fig. 8). At the end of spring, on 9 June 2008 (post blooms period), the biological origin of the major fluorophore released (peak T, tryptophan-like) was logically dominated by bacteria at 2 and 5 m depth at SOFCOM station.

At the beginning of summer (23 June 2008 sample) during an important surface extent of the Rhône River plume in the Bay of Marseilles, CDOM exhibited an absorption coefficient in the upper range with the highest spectral slope (Table 2), comparable to

BGD
7, 5675–5718, 2010

those generally observed in open ocean (Blough and Del Vecchio, 2002). In addition, high fluorescence intensities for all peaks (T, M, C, and B) (Table 3), as well as fluorescence indices values (HIX, BIX and M/C) (Table 4) indicated a well developed surface biological activity that produced fresh fluorescent CDOM especially at 2 m but also at 5 m depth. Moreover, the biological origin of tryptophan released was controlled mostly by phytoplankton at both depths.

Two weeks after this important bloom, on 10 July 2008, bacteria dominated the biological input of tryptophan at 5 m depth. On this date, the autochthonous production of CDOM was weak while S_{CDOM} was high despite a minor mixing event that probably injected nutrients and humic CDOM into surface waters (Fig. 8). This could explain the significant values of HIX and BIX. Nevertheless, low $a_{CDOM}(350)$ coupled to a high S_{CDOM} also point out the efficiency of photobleaching effect of CDOM in this area and could explain its net loss observed on 10 July 2008 at both depths.

During summer time, under any influence of Rhône River plume in this area, photobleaching appeared as a significant sink for CDOM (Fig. 8). This process was most clearly illustrated at the end of summer time, on 23 September 2008, with respect to the quality and quantity of CDOM content. Indeed, on 23 September 2008 the warm and salty water mass present had persisted at the surface since late July (Fig. 2) and had thus spent 6–8 weeks exposed to high UV radiation. Values of $a_{CDOM}(350)$ exhibited minima at both depths and high spectral slopes were high especially at 5 m depth where the water was saltiest (Table 2). Moreover, EEMs illustrated a strong signal of fluorescence in short Ex/Em wavelengths (Figs. 4 and 5), which was attributed to photobleaching. Thus, it was logical that the most important net loss of CDOM due to photobleaching appeared at the end of summer time just before fall mixing.

Finally, during fall, on 25 November 2008, 12 consecutive days of Mistral wind enhanced strong deep mixing that put nutrients back in the surface waters as well humic CDOM, from deep water (Coble, 1998; Sierra et al., 1997; 2005; Komada et al., 2002) (Fig. 8). The maximum of value for peak C was observed on this date (Table 3). Maximum values for autochthonous humic CDOM (peak M) were also observed at this

BGD
7, 5675–5718, 2010

time, probably of bacterial origin (Nieto-Cid et al., 2006). Therefore, the inputs of humic CDOM (peaks C and M) explain the highest $a_{CDOM}(350)$ and the lowest spectral slope of CDOM observed at both depths during this period.

5 Conclusions and perspectives

This study highlights the low surface CDOM content in the Bay of Marseilles through $a_{CDOM}(350)$ and TOC concentration values. Stable and very low annual mean value of $a_{CDOM}(350)$ prevents the establishment of a seasonal trend, while S_{CDOM} values were significantly higher during the summer time period and thus could reflect either photobleaching or biological production of CDOM in the surface waters. Values of $a_{CDOM}(350)$ in this well-urbanized coastal area were comparable to those usually found in the open ocean. The different fluorophores identified in this study show the predominance of protein-like component, peak T, and marine humic-like component, peak M. The omnipresence of these fluorescent peaks is related to the biological activity occurring mainly in the surface waters of the Bay of Marseilles. The very low content in UVA humic-like peak C demonstrates the quasi absence of terrestrial material within fluorescent CDOM composition. According to the common use, as Marseilles Bay optical properties of water were governed mostly by phytoplankton with their accompanying by-products and the terrigeneous influence is negligible, therefore waters in this coastal area belong to case 1 waters.

This study points out for the first time that the surface waters of the Bay of Marseilles are influenced by episodic events of the eastward extent of the Rhône plume. In this coastal oligotrophic area, these events enhance surface primary production and bacterial activity in surroundings waters which in turn increase the surface CDOM production. This source of CDOM appears more efficient at 2 m compared at 5 m depth and during water stratification. On the other side, photobleaching acts as a significant sink of CDOM in summer, whereas the mixing of bottom waters containing humic CDOM may enrich the surface waters.

BGD
7, 5675–5718, 2010

From the results presented in this work, it appears clearly that the Rhône River plume intrusions as well as mixing of the water column have a significant impact on the biogeochemical cycles in the Bay of Marseilles. Determining photobleaching rates of surface CDOM appears also as an important issue. A higher temporal determination of these processes in this coastal area will enable a better understanding of the biogeochemical/physical processes driving the CDOM distribution, dynamics and fate in the Marseilles Bay and will shed light on some features, not observed in this study, such as interseasonal trend of CDOM, and relationships between fluorescence, absorbance and DOC concentration, commonly observed in coastal area.

Acknowledgements. This work was supported by the French ANR-06-VULN-001 to the CHACCRA project supervised by C. Rabouille, INSU/CNRS as well as Conseil Général des Bouches du Rhône (CG13) and Pôle Mer PACA funding UVPACA project (PI: B. Charrière). This study partly contributes to "Sea Explorer" project supported by the French "Fond de Compétitivité des Entreprises" and Pôle Mer PACA. We are very grateful to the crews of the R/V Antedon II and Tethys II for their excellent service at sea and the SO-COM staff for providing CTD data from SOFCOM station and for collecting Rhône River samples at Arles station. We thank IFREMER for providing ocean color data through the website http://www.ifremer.fr/nausicaa/medit/index.htm. We are grateful to M. Goutx for the use of the Hitachi spectrofluorometer. PhD scholarship to J. Para was provided by PACA region, whereas visiting professor fellowship to P. Coble was provided by Université de la Méditerranée.

The publication of this article is financed by CNRS-INSU.

References

Arnoux-Chiavassa, S., Rey, V., and Fraunié, P.: Modeling 3-D Rhone River plume using a higher order advection scheme, Oceanol. Acta, 26, 299–309, 2003.

Azam, F., Fenchel, T., Field, J. G., Gray, J. S., Meyer-Reil, L. A., and Thingstad, F.: The ecological role of water-column microbes in the sea, Mar. Ecol.-Prog. Ser., 10, 257–263, 1983.

Babin, M., Stramski, D., Ferrari, G. M., Claustre, H., Bricaud, A., Obolensky, G., and Hoepffner, N.: Variations in the light absorption coefficients of phytoplankton, non-algal particles, and dissolved organic matter in coastal waters around Europe, J. Geophys. Res., 108(C7), 3211, 2003.

Belzile, C., Roesler, C. S., Christensen, J. P., Shakhova, N., and Semiletov, I.: Fluorescence measured using the WETStar DOM fluorometer as a proxy for dissolved matter absorption, Estuar. Coast. Shelf S., 67, 441–449, 2006.

Blough, N. V., Zafiriou, O. C., and Bonilla, J.: Optical absorption spectra of water from the Orinoco River outflow: terrestrial input of colored organic matter to the Caribbean, J. Geophys. Res., 98(C2), 2271–2278, 1993.

Blough, N. V. and Del Vecchio, R.: Chromophoric DOM in the coastal environment, in: Biogeochemistry of Marine Dissolved Organic Matter, edited by: Hansell, D. A. and Carlson, C. A., Academic Press, San Diego, 509–540, 2002.

Brasseur, P., Beckers, J. M., Brankart, J. M., and Schoenauen, R.: Seasonal temperature and salinity fields in the Mediterranean Sea: climatological analyses of a historical data set, Deep-Sea Res. Pt. I, 43, 159–192, 1996.

Bricaud, A., Morel, A., and Prieur, L.: Absorption by dissolved organic matter of the sea (yellow substance) in the UV and visible domains, Limnol. Oceanogr., 26, 43–53, 1981.

Broche, P., Devenon, J. L., Forget, P., De Maistre, J. C., Naudin, J. J., and Cauwet, G.: Experimental study of the Rhone plume. Part I: physics and dynamics, Oceanol. Acta, 21, 725–738, 1998.

Coble, P. G., Green, S. A., Blough, N. V., and Gagosian, R. B.: Characterisation of dissolved organic matter in the Black Sea by fluorescence spectroscopy, Nature, 348, 432–435, 1990.

Coble, P. G., Schultz, C. A., and Mopper, K.: Fluorescence contouring analysis of DOC intercalibration experiments samples: a comparison of techniques, Mar. Chem., 41, 173–178, 1993.

Coble, P. G.: Characterization of marine and terrestrial DOM in seawater using excitation emis-

BGD
7, 5675–5718, 2010

sion matrix spectroscopy, Mar. Chem., 51, 325–346, 1996.
Coble, P. G., Del Castillo, C. E., and Avril, B.: Distribution and optical properties of CDOM in the Arabian Sea during the 1995 southwest monsoon, Deep-Sea Res. Pt. II, 45, 2195–2223, 1998.
Coble, P. G.: Marine optical biogeochemistry: the chemistry of ocean color, Chem. Rev., 107, 402–418, 2007.
Cristofanelli, P. and Bonasoni, P.: Background ozone in the Southern Europe and Mediterranean area: influence of the transport processes, Environ. Pollut., 157, 1399–1406, 2009.
Cruzado, A. and Velasquez, Z. R.: Nutrients and phytoplankton in the Gulf of Lions, Cont. Shelf. Res., 10, 931–942, 1990.
D'Sa, E. J., Steward, R. G., Vodacek, A., Blough, N. V., and Phinney, D.: Determining optical absorption of colored dissolved organic matter in seawater with a liquid capillary waveguide, Limnol. Oceanogr., 44, 4, 1142–1148, 1999.
Dafner, E. V., Sempéré, R., and Bryden, H. L.: Total organic carbon distribution and budget through the Strait of Gibraltar in April 1998, Mar. Chem., 73, 233–252, 2001.
De Souza-Sierra, M. M., Donard, O. F. X., Lamotte, M., Belin, C., and Ewald, M.: Fluorescence spectroscopy of coastal and marine waters, Mar. Chem., 47, 127–144, 1994.
Del Castillo, C. E., Coble, P. G., Morell, J. M., Lopez, J. M., and Corredor, J. E.: Analysis of the optical properties of the Orinoco River plume by absorption and fluorescence spectroscopy, Mar. Chem., 66, 35–51, 1999.
Del Castillo, C. E., Coble, P. G., and Müller-Karger, F. E.: On the dispersal of riverine colored dissolved organic matter over the West Florida Shelf, Limnol. Oceanogr., 45, 1452–1432, 2000.
Del Vecchio, R. and Blough, N. V.: On the origin of the optical properties of humic substances, Environ. Sci. Technol., 38, 3885–3891, 2004.
Determann, S., Reuter, R., Wagner, P., and Willkomm, R.: Fluorescence matter in the Eastern Atlantic Ocean. Part 1: method of measurement and near-surface distribution, Deep-Sea Res., 41, 659–675, 1994.
Determann, S., Reuter, R., and Willkomm, R.: Fluorescent matter in the Eastern Atlantic Ocean. Part 2: vertical profiles and relation to water masses, Deep-Sea Res., 43, 345–360, 1996.
Determann, S., Lobbes, J. M., Reuter, R., and Rullkötter, J.: Ultraviolet fluorescence excitation and emission spectroscopy of marine algae and bacteria, Mar. Chem., 62, 137–156, 1998.

BGD
7, 5675–5718, 2010

Devenon, J. L., Broche, P., De Maistre, J. C., Forget, P., Gagelli, J., and Rougier, G.: VHF radar measurements in the Rhone River plume, Water Pol. R., 28, 75–87, 1992.
Doval, M. D., Pérez, F. F., and Berdalet, E.: Dissolved and particulate organic carbon and nitrogen in the Northwestern Mediterranean, Deep-Sea Res. Pt. I, 46, 511–527, 1999.
Durrieu de Madron, X., Denis, L., Diaz, F., Garcia, N., Guieu, C., Grenz, C., Loyë-Pilot, M. D., Ludwig, W., Moutin, T., Raimbault, P., and Ridame, C.: Nutrients and carbon budgets for the Gulf of Lion during the Moogli cruises, Oceanol. Acta, 26, 421–433, 2003.
Estournel, C., Broche, P., Marsaleix, P., Devenon, J. L., Auclair, F., and Vehil, R.: The Rhone River plume in unsteady conditions: numerical and experimental results, Estuar. Coast. Shelf S., 53, 25–38, 2001.
Ferrari, G. M.: The relationship between chromophoric dissolved organic matter and dissolved organic carbon in the European Atlantic coastal area and in the West Mediterranean Sea (Gulf of Lions), Mar. Chem., 70, 339–357, 2000.
Fontana, C., Grenz, C., Pinazo, C., Marsaleix, P., and Diaz, F.: Assimilation of SeaWiFS chlorophyll data into a 3-D-coupled physical-biogeochemical model applied to a freshwater-influenced coastal zone, Cont. Shelf Res., 29 (11–12), 1397–1409, 2009.
Fontana, C., Grenz, C., and Pinazo, C.: Sequential assimilation of a year-long time-series of SeaWiFS chlorophyll data on the French Mediterranean coast, Cont. Shelf Res., in review., 2010.
Forget, P., Devenon, J. L., De Maistre, J. C., Broche, P., and Leveau, M.: VHF remote sensing for mapping river plume circulation, Geophys. Res. Lett., 17, 1097–1100, 1990.
Gatti, J., Petrenko, A., Devenon, J. L., Leredde, Y., and Ulses, C.: The Rhone River dilution zone present in the northeastern shelf of the Gulf of Lion in December 2003, Cont. Shelf Res., 26, 1794–1805, 2006.
Gohin, F., Druon, J. N., and Lampert, L.: A five channel chlorophyll concentration algorithm applied to SeaWiFS data processed by SeaDAS in coastal waters, Int. J. Remote Sens., 23(8), 1639–1661, 2002.
Gohin, F., Loyer, S., Lunven, M., Labry, C., Froidefond, J. M., Delmas, D., Huret, M., and Herbland, A.: Satellite-derived parameters for biological modelling in coastal waters: illustration over the eastern continental shelf of the Bay of Biscay, Remote Sens. Environ., 95(1), 29–46, 2005.
Green, S. A. and Blough, N. V.: Optical absorption and fluorescence properties of chromophoric dissolved organic matter in natural waters, Limnol. Oceanogr., 39, 1903–1916, 1994.

BGD
7, 5675–5718, 2010

Grzybowski, W.: Effect of short-term irradiation on the absorbance spectra of the chromophoric organic matter dissolved in the coastal and riverine waters, Chemosphere, 40, 1313–1318, 2000.
Hedges, J. I.: Global biogeochemical cycles: Progress and problems, Mar. Chem., 39, 67–93, 1992.
Hedges, J. I.: Why dissolved organics matter?, in: Biogeochemistry of Marine Dissolved Organic Matter, edited by: Hansell, D. A. and Carlson, C. A., Academic Press, San Diego, 1–27, 2002.
Højerslev, N. K., Holt, N., and Aarup, T.: Optical measurements in the North Sea-Baltic Sea transition zone. I. On the origin of the deep water in the Kattegat, Cont. Shelf Res., 16(10), 1329–1342, 1996.
Huguet, A., Vacher, L., Relexans, S., Saubusse, S., Froidefond, J. M., and Parlanti, E.: Properties of fluorescent dissolved organic matter in the Gironde Estuary, Org. Geochem., 40, 706–719, 2009.
Jerlov, N. G.: Optical Oceanography, American Elsevier Publ. Co., Inc., New York, 1968.
Joux, F., Jeffrey, W. H., Abboudi, M., Neveux, J., Pujo-Pay, M., Oriol, L., and Naudin, J. J.: Ultraviolet radiation in the Rhône River lenses of low-salinity and in marine waters of the Northwestern Mediterranean Sea: attenuation and effects on bacterial activities and net community production, Photochem. Photobiol., 85, 783–793, 2009.
Kirk, J. T. O.: Light and Photosynthesis in Aquatic Ecosystems, 2nd edn., Cambridge University Press, Cambridge, 1994.
Komada, T., Shofield, O. M. E., and Reimers, C. E.: Fluorescence characteristics of organic matter released from coastal sediments during resuspension, Mar. Chem., 79, 81–97, 2002.
Margat, J.: L'eau dans le basin de la méditerranéen, situation et prospective, in: Les Fascicules du Plan Bleu, Vol. 6, Economica, Paris, 1992.
Mayer, L. M., Schick, L. L., and Loder III, T. C.: Dissolved protein fluorescence in two Maine estuaries, Mar. Chem., 64, 171–179, 1999.
The MERMEX group: Marine Ecosystems Responses to climatic and anthropogenic forcings in the Mediterranean, submitted to Prog. Oceanogr., 2010.
Mopper, K. and Schultz, C. A.: Fluorescence as a possible tool for studying the nature and water column distribution of DOC components, Mar. Chem., 41, 229–238, 1993.
Mopper, K. and Kieber, D. J.: Marine photochemistry and its impact on carbon cycling, in: The Effects of UV Radiation in the Marine Environment, edited by: de Mora, S., Demers, S., and

BGD
7, 5675–5718, 2010

Vernet, M., Cambridge University Press, Cambridge, 101–129, 2000.
Mopper, K. and Kieber, D. J.: Photochemistry and the cycling of carbon, sulphur, nitrogen and phosphorus, in: Biogeochemistry of Marine Dissolved Organic Matter, edited by: Hansell, D. A. and Carlson, C. A., Academic Press, San Diego, 455–507, 2002.
Moran, M. A., Sheldon Jr., W. M, and Zepp, R. G.: Carbon loss and optical property change during long term photochemical and biological degradation of estuarine dissolved organic matter, Limnol. Oceanogr., 45(6), 1254–1264, 2000.
Mueller, J. L. and Austin, R. W.: Ocean Optics Protocols for SeaWiFS Validation, Revision 1. NASA Tech. Memo. 104566, Vol. 25, edited by: Hooker, S. B., Firestone, E. R., and Acker, J. G., NASA GSFC, Greenbelt, Maryland, 67 pp., 1995.
Myklestad, S. M.: Dissolved organic carbon from phytoplankton, in: The Handbook of Environmental Chemistry, edited by: Wangersky, P., 5(D), Mar. Chem., 111–148, Springer-Verlag Berlin/Heidelberg, Heidelberg, 2000.
Nelson, J. R. and Guarda, S.: Particulate and dissolved spectral absorption on the continental shelf of the Southeastern United States, J. Geophys. Res., 100, 8715–8732, 1995.
Nelson, N. B., Siegel, D. A., and Michaels, A. E.: Seasonal dynamics of colored dissolved material in the Sargasso Sea, Deep-Sea Res. Pt. I, 45, 931–957, 1998.
Nelson, N. B. and Siegel, D. A.: Chromophoric DOM in the open ocean, in: Biogeochemistry of Marine Dissolved Organic Matter, edited by: Hansell, D. A. and Carlson, C. A., Academic Press, San Diego, 547–578, 2002.
Nelson, N. B., Carlson, C. A., and Steinberg, D. K.: Production of chromophoric dissolved organic matter by Sargasso Sea microbes, Mar. Chem., 89, 273–287, 2004.
Nelson, N. B., Siegel, D. A., Carlson, C. A., Swan, C., Smethie Jr., W. M., and Khatiwala, S.: Hydrography of chromophoric dissolved organic matter in the North Atlantic, Deep-Sea Res. Pt. I, 54, 710–731, 2007.
Nieke, B., Reuter, R., Heuermann, R., Wang, H., Babin, M., and Therriault, J. C.: Light absorption and fluorescence properties of chromophoric dissolved organic matter (CDOM) in the St. Lawrence Estuary (Case 2 waters), Cont. Shelf Res., 17, 235–252, 1997.
Nieto-Cid, M., Alvarez-Salgado, X. A., and Perez, F.: Microbial and photochemical reactivity of fluorescent dissolved organic matter in a coastal upwelling system, Limnol. Oceanogr., 51, 1391–1400, 2006.
Opsahl, S. and Benner, R.: Distribution and cycling of terrigenous dissolved organic matter in the ocean, Nature, 386, 480–482, 1997.

BGD
7, 5675–5718, 2010

Pujo-Pay, M., Conan, P., Joux, F., Oriol, L., Naudin, J. J., and Cauwet, G.: Impact of phytoplankton and bacterial production on nutrient and DOM uptake in the Rhône River plume (NW Mediterranean), Mar. Ecol.-Prog. Ser., 315, 43–54, 2006.
Reffray, G., Fraunié , P., and Marsaleix, P.: Secondary flows induced by wind forcing in the Rhône region of freshwater influence, Ocean Dynam., 54, 179–196, 2004.
Romera-Castillo, C., Sarmento, H., Alvarez-Salgado, X. A., Gasol, J. M., and Marrasé, C.: Production of chromophoric dissolved organic matter by marine phytoplankton, Limnol. Oceanogr., 55, 446–454, 2010.
Ruiz, S., Gomis, D., Sotillo, M. G., and Josey, S. A: Characterization of surface heat fuxes in the Mediterranean Sea from a 44-year high-resolution atmospheric data set, Global. Planet. Change, 63, 258–274, 2008.
Santinelli, C., Gasparini, G. P., Nannicini, L., and Seritti, A.: Vertical distribution of dissolved organic carbon (DOC) in the Western Mediterranean Sea, Deep-Sea Res. Pt. I, 49, 2203–2219, 2002.
Seckmeyer, G., Pissulla, D., Glandorf, M., Henriques, D., Johnsen, B., Webb, A., Siani, A. M., Bais, A., Kjeldstad, B., Brogniez, C., Lenoble, J., Gardiner, B., Kirsch, P., Koskela, T., Kaurola, J., Uhlmann, B., Slaper, H., den Outer, P., Janouch, M., Werle, P., Gröbner, J., Mayer, B., de la Casiniere, A., Simic, S., and Carvalho, F.: Variability of UV irradiance in Europe, Photochem. Photobiol, 84, 172–179, 2008.
Sempéré, R., Charrière, B., Cauwet, G., and Van-Wambeke, F.: Carbon inputs of the Rhône River to the Mediterranean Sea: biogeochemical implications, Global Biogeochem. Cy., 14(2), 669–681, 2000.
Sempéré, R., Panagiotopoulos, C., Lafont, R., Marroni, B., and Van Wambeke, F.: Total organic carbon dynamics in the Aegean Sea, J. Marine Syst., 33–34, 355–364, 2002.
Seritti, A., Russo, D., Nannicini, L., and Del Vecchio, R.: DOC, absorption and fluorescence properties of estuarine and coastal waters of the Northern Tyrrhenian Sea, Chem. Spec. Bioavailab., 10, 95–105, 1998.
Seritti, A., Manca, B. B., Santinelli, C., Murru, E., Boldrin, A., and Nannicini, L.: Relationships between hydrological properties and dissolved organic carbon (DOC) in the Ionian Sea (winter 1999), J. Geophys. Res.-Oceans, 108, 8112, doi:10.1029/2002JC001345, 2003.
Siegel, D. A., Maritorena, S., Nelson, N. B., Hansell, D. A., and Lorenzi-Kayser, M.: Global distribution and dynamics of colored dissolved and detrital organic materials, J. Geophys. Res., 107(C12), 3228, 2002.

BGD
7, 5675–5718, 2010

Sierra, M. M. D., Donard, O. F. X., and Lamotte, M.: Behaviour of dissolved fluorescent organic matter during estuarine mixing, Mar. Chem., 58, 51–58, 1997.
Sierra, M. M. D., Giovanela, M., Parlanti, E., and Soriano-Sierra, E. J.: Fluorescence fingerprint of fulvic and humic acids from varied origins as viewed by single-scan and excitation/emission matrix techniques, Chemosphere, 58, 715–733, 2005.
Sohrin, R. and Sempéré, R.: Seasonal variation in total organic carbon in the Northeast Atlantic in 2000–2001, J. Geophys. Res., 110, C10S90, doi:10.1029/2004JC002731, 2005.
Smith, S. V. and Hollibaugh, J. T.: Coastal metabolism and the oceanic organic carbon balance, Rev. Geophys., 31, 75–89, 1993.
Stedmon, C. A., Markager, S., and Kaas, H.: Optical properties and signatures of chromophoric dissolved organic matter (CDOM) in Danish coastal waters, Estuar. Coast. Shelf S., 51, 267–278, 2000.
Stedmon, C. A. and Markager, S.: Tracing the production and degradation of autochthonous fractions of dissolved organic matter using fluorescence analysis, Limnol. Oceanogr., 50, 1415–1426, 2005.
Tedetti, M. and Sempéré, R.: Penetration of UV radiation in the marine environment: a review, Photochem. Photobiol., 82, 389–397, 2006.
Tedetti, M., Guigue, C., and Goutx, M.: Utilization of a submersible UV fluorometer for monitoring anthropogenic inputs in the Mediterranean coastal waters, Mar. Pollut. Bull., 60, 350–362, 2010.
Vähätalo, A. V. and Wetzel, R. G.: Photochemical and microbial decomposition of chromophoric dissolved organic matter during long (months-years) exposures, Mar. Chem., 89, 313–326, 2004.
Vasilkov, A., Krotkov, N., Herman, J., McClain, C., Arrigo, K., and Robinson, W.: Global mapping of underwater UV irradiances and DNA-weighted exposures using Total Ozone Mapping Spectrometer and Sea-viewing Wide Field-of-view Sensor data products, J. Geophys. Res., 106, 27205–27219, 2001.
Vignudelli, S., Santinelli, C., Murru, E., Nannicini, L., and Seritti, A.: Distributions of dissolved organic carbon (DOC) and chromophoric dissolved organic matter (CDOM) in coastal waters of the Northern Tyrrhenian Sea (Italy), Estuar. Coast. Shelf S., 60, 133–149, 2004.
Vodacek, A., Blough, N. V., DeGrandpre, M. D., Peltzer, E. T., and Nelson, R. K.: Seasonal variation of CDOM and DOC in the Middle Atlantic Bight: terrestrial inputs and photooxidation, Limnol. Oceanogr., 42(2), 674–686, 1997.

BGD
7, 5675–5718, 2010

Yamashita, Y. and Tanoue, E.: Chemical characterization of protein-like fluorophores in DOM in relation to aromatic amino acids, Mar. Chem., 82, 255–271, 2003.
Zsolnay, A., Baigar, E., Jimenez, M., Steinweg, B., and Saccomandi, F.: Differentiating with fluorescence spectroscopy the sources of dissolved organic matter in soils subjected to drying, Chemosphere, 38, 45–50, 1999.

BGD
7, 5675–5718, 2010

Table 1. Sampling dates at SOFCOM station (5° 17′ 30″ E; 43° 14′ 30″ N), Rhône estuary stations (4° 52′ 42″ E; 43° 12′ 6″ N and 4° 51′ 25″ E; 43° 12′ 90″ N) and at Arles station (Rhône) with corresponding parameters available (×) or not (–). Absorption coefficient of CDOM at 350 nm [$a_{CDOM}(350)$], spectral slope of CDOM determined on the 350–500 nm range with a non linear regression (S_{CDOM}), total organic carbon (TOC) concentration , chlorophyll-*a* concentration (Chl-*a*), at 2 and 5 m depths and mean surface irradiance (E_s) in the UVB (305 nm) and UVA (325, 340, 380 nm) spectral domains measured during one hour close to solar noon on ship deck.

End-member	Date	Season	a_{CDOM}	S_{CDOM}	EEM	TOC	Chl-*a*	E_s(UV)
SOFCOM	7 Nov 2007	fall	×	×	–	×	–	×
SOFCOM	19 Dec 2007	winter	×	×	–	×	–	×
SOFCOM	5 Feb 2008	winter	×	×	–	×	×	×
SOFCOM	14 Feb 2008	winter	×	×	–	×	×	×
SOFCOM	26 Mar 2008	spring	×	×	–	×	×	×
SOFCOM	29 Apr 2008	spring	×	×	–	×	×	×
SOFCOM	6 May 2008	spring	×	×	–	×	×	×
SOFCOM	9 Jun 2008	spring	×	×	×	×	×	×
SOFCOM	23 Jun 2008	summer	×	×	×	×	×	×
SOFCOM	10 Jul 2008	summer	×	×	×	×	×	×
SOFCOM	23 Sep 2008	summer	×	×	×	×	×	×
SOFCOM	14 Oct 2008	fall	×	×	×	×	×	×
SOFCOM	25 Nov 2008	fall	×	×	×	×	×	×
SOFCOM	4 Dec 2008	fall	×	×	×	×	×	×
Rhône estuary	22 May 2008	spring	×	×	–	×	–	–
Rhône estuary	23 May 2008	spring	×	×	–	×	–	–
Rhône (Arles) (n=14)	17 Jan 2008–18 Nov 2008	–	×	×	Jun 2008–Dec 2008	×	–	–
Rhône (Arles) (n=4)	27 May 2008–1 Jul 2008	spring-summer	×	×	×	×	–	–

BGD
7, 5675–5718, 2010

Table 2. Absorption coefficient of CDOM at 350 nm [$a_{CDOM}(350)$], spectral slope of CDOM (S_{CDOM}) determined on the 350–500 nm range with a non linear regression, total organic carbon (TOC) concentration, chlorophyll-*a* concentration (Chl-*a*) at 2 and 5 m depths and mean surface irradiance (E_s) in the UVB (305 nm) and UVA (325, 340, 380 nm) spectral domains measured during one hour close to solar noon on ship deck.

End-member	Date	$a_{CDOM}(350)$ [m^{-1}]		S_{CDOM} [nm^{-1}]		TOC [µM C]		Chl-*a* [µg l^{-1}]		E_s(UV) [µW cm^{-2} nm^{-1}]			
		2 m	5 m	2 m	5 m	2 m	5 m	2 m	5 m	305 nm	325 nm	340 nm	380 nm
SOFCOM [a]	7 Nov 2007	0.11	0.10	0.018	0.019	68	62	–	–	0.51 ± 0.03	12.78 ± 0.39	20.74 ± 0.59	29.17 ± 0.73
SOFCOM	19 Dec 2007	0.10	0.10	0.017	0.018	60	54	–	–	0.14 ± 0.01	9.49 ± 0.06	17.13 ± 0.11	26.46 ± 0.11
SOFCOM	5 Feb 2008	0.11	0.11	0.016	0.015	–	55	0.90	0.92	0.48 ± 0.10	15.72 ± 0.09	25.56 ± 0.17	36.19 ± 0.38
SOFCOM	14 Feb 2008	0.09	0.09	0.018	0.018	78	61	0.20	1.03	0.42 ± 0.01	16.86 ± 0.08	27.90 ± 0.19	38.81 ± 0.23
SOFCOM [a]	26 Mar 2008	–	0.10	–	0.016	56	59	0.21	0.24	1.39 ± 0.03	25.85 ± 0.34	39.09 ± 0.61	52.86 ± 0.98
SOFCOM	29 Apr 2008	0.11	0.11	0.018	0.020	70	63	0.85	0.89	3.09 ± 0.09	36.62 ± 1.25	54.67 ± 2.29	74.18 ± 3.17
SOFCOM [a]	6 May 2008	0.13	0.13	0.018	0.018	65	–	1.55	1.69	0.93 ± 0.05	12.83 ± 0.72	18.81 ± 1.08	24.47 ± 1.48
SOFCOM [a]	9 Jun 2008	0.11	0.10	0.022	0.023	70	61	0.77	0.86	2.26 ± 0.09	27.87 ± 1.07	40.55 ± 1.65	53.69 ± 2.57
SOFCOM	23 Jun 2008	0.12	0.11	0.026	0.026	79	76	1.42	1.33	4.64 ± 0.06	39.14 ± 0.25	56.51 ± 0.43	77.51 ± 0.81
SOFCOM [b]	10 Jul 2008	0.09	0.09	0.023	0.023	67	68	0.19	0.20	4.06 ± 0.09	40.14 ± 0.92	58.88 ± 1.35	79.62 ± 1.69
SOFCOM [a]	23 Sep 2008	0.07	0.06	0.021	0.023	72	67	0.40	0.45	1.13 ± 0.12	15.92 ± 1.64	23.38 ± 2.62	30.98 ± 4.06
SOFCOM [b]	14 Oct 2008	0.09	0.09	0.018	0.018	70	67	0.33	0.35	1.17 ± 0.01	19.58 ± 0.08	30.08 ± 0.27	43.75 ± 0.51
SOFCOM	25 Nov 2008	0.13	0.13	0.014	0.014	55	56	0.58	0.56	0.32 ± 0.01	13.73 ± 0.01	22.88 ± 0.01	33.78 ± 0.01
SOFCOM [a]	4 Dec 2008	0.11	0.10	0.017	0.019	63	65	0.76	0.96	0.18 ± 0.01	7.34 ± 0.30	11.65 ± 0.48	15.28 ± 0.62
Rhône estuary [c]	22 May 2008	0.25	0.09	0.019	0.021	74	71	–	–	–	–	–	–
Rhône estuary [c]	23 May 2008	0.33	0.09	0.017	0.024	78	67	–	–	–	–	–	–
Rhône (Arles) (n=14) [c]	17 Jan 2008–18 Nov 2008	2.42 ± 1.05	–	0.017 ± 0.001	–	136 ± 38	–	–	–	–	–	–	–
Rhône (Arles) (n=4) [c]	27 May 2008–1 Jul 2008	1.65 ± 0.53	–	0.017 ± 0.001	–	103 ± 18	–	–	–	–	–	–	–

[a] Cloudy day
[b] Sea mist
[c] For Rhône estuary, and Rhône end-members DOC concentration was measured in place of TOC concentration.

BGD
7, 5675–5718, 2010

Table 3. Fluorescence intensity (in QSU) and peak positions of tyrosine-like (B), tryptophan-like (T), UVA humic-like (C) and marine humic-like (M) observed at SOFCOM station at 2 and 5 m depths. Emission ranges represent the band from which a mean of fluorescence intensity was calculated. Peak B was not detectable (nd) except on 23 June 2008.

	Peak fluorescence intensity (QSU)							
	B		C		M		T	
	Ex/Em (nm)=275/300–310		Ex/Em (nm)=350/430–450		Ex/Em (nm)=300/380–400		Ex/Em (nm)=275/330–350	
Date	2 m	5 m	2 m	5 m	2 m	5 m	2 m	5 m
9 Jun 2008	nd	nd	0.56 ± 0.04	0.57 ± 0.04	1.02 ± 0.06	1.24 ± 0.08	1.70 ± 0.18	1.74 ± 0.13
23 Jun 2008	11.06 ± 0.81	3.51 ± 0.67	1.40 ± 0.06	1.54 ± 0.08	4.34 ± 0.13	2.73 ± 0.12	14.13 ± 1.57	3.78 ± 0.20
10 Jul 2008	nd	nd	0.49 ± 0.03	0.51 ± 0.04	0.85 ± 0.06	0.96 ± 0.06	1.25 ± 0.13	1.46 ± 0.09
23 Sep 2008	nd	nd	0.57 ± 0.04	0.42 ± 0.03	1.26 ± 0.07	0.90 ± 0.09	2.77 ± 0.20	1.87 ± 0.09
14 Oct 2008	nd	nd	nd	0.27 ± 0.03	nd	0.55 ± 0.08	1.30 ± 0.18	1.58 ± 0.17
25 Nov 2008	nd	nd	2.99 ± 0.18	2.85 ± 0.22	5.82 ± 0.49	5.11 ± 0.52	21.94 ± 2.66	nd
4 Dec 2008	nd	nd	0.59 ± 0.04	0.34 ± 0.03	0.98 ± 0.05	0.71 ± 0.07	2.08 ± 0.18	nd
Mean	–	–	1.10	0.93	2.38	1.74	6.45	1.94
SD	–	–	*0.99*	*0.95*	*2.15*	*1.65*	*8.25*	*0.93*

BGD
7, 5675–5718, 2010

Table 4. Values of Humification (HIX; Zsolnay et al., 1999), Biological (BIX; Huguet et al., 2009) indices and the ratio of marine humic-like (Ex/Em=300/380–400 nm) to humic like (Ex/Em=350/430–450 nm) (M/C) fluorescence at SOFCOM station at 2 and 5 m depths.

	HIX		BIX		M/C	
Date	2 m	5 m	2 m	5 m	2 m	5 m
9 Jun 2008	0.93	0.96	1.35	1.35	1.81	2.17
23 Jun 2008	0.42	1.22	1.47	1.26	3.11	1.77
10 Jul 2008	1.32	1.35	1.23	1.40	1.74	1.89
23 Sep 2008	1.04	0.96	1.23	1.13	2.22	2.12
14 Oct 2008	nd	0.27	nd	1.19	nd	2.08
25 Nov 2008	1.01	0.77	1.60	1.33	1.95	1.79
4 Dec 2008	0.35	0.76	1.32	1.29	1.68	2.08
Mean	0.84	0.90	1.37	1.28	2.09	1.99
SD	*0.38*	*0.35*	*0.15*	*0.09*	*0.54*	*0.17*

BGD
7, 5675–5718, 2010

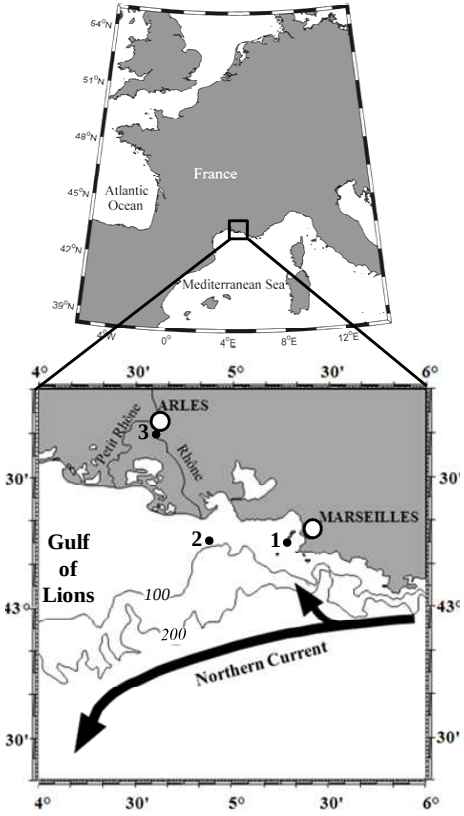

Fig. 1. Map of the Bay of Marseilles marking the location of SOFCOM station (black dot 1) in the Bay of Marseilles, the two Rhône estuary stations (black dot 2) and Arles station (black dot 3). Distance separating SOFCOM station from Rhône River estuary is around 40 km.

BGD
7, 5675–5718, 2010

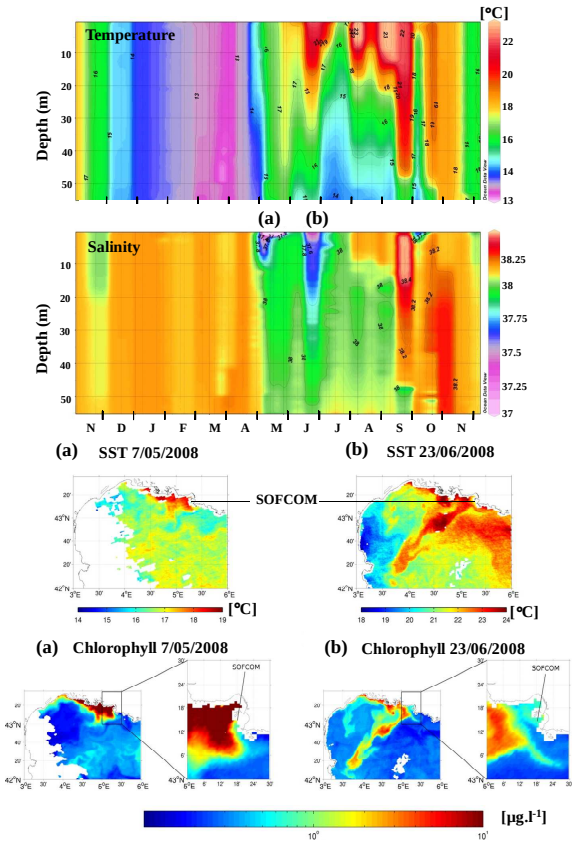

Fig. 2. Top panels: temporal evolution of temperature and salinity at SOFCOM station from Nov 2007 to Dec 2008 from surface to bottom. Data come from CTD profiles carried out twice a month by the SOMLIT network (n=30) and completed since Feb 2008 by CTD data acquired on sampling dates (n=11). Bottom panels: remotely sea surface temperature (SST) and chlorophyll concentrations are from the points in the time series labeled **(a)** and **(b)** corresponding, respectively to the sampling date 7 May 2008 and 23 June 2008. Remotely SST and chlorophyll concentrations from satellite images were obtained, respectively by applying the long-wave SST algorithm and the OC5 coastal-oriented optical algorithm (Gohin et al., 2002, 2005) to water leaving irradiances derived from the Moderate Resolution Imaging Spectroradiometer (MODIS).

BGD
7, 5675–5718, 2010

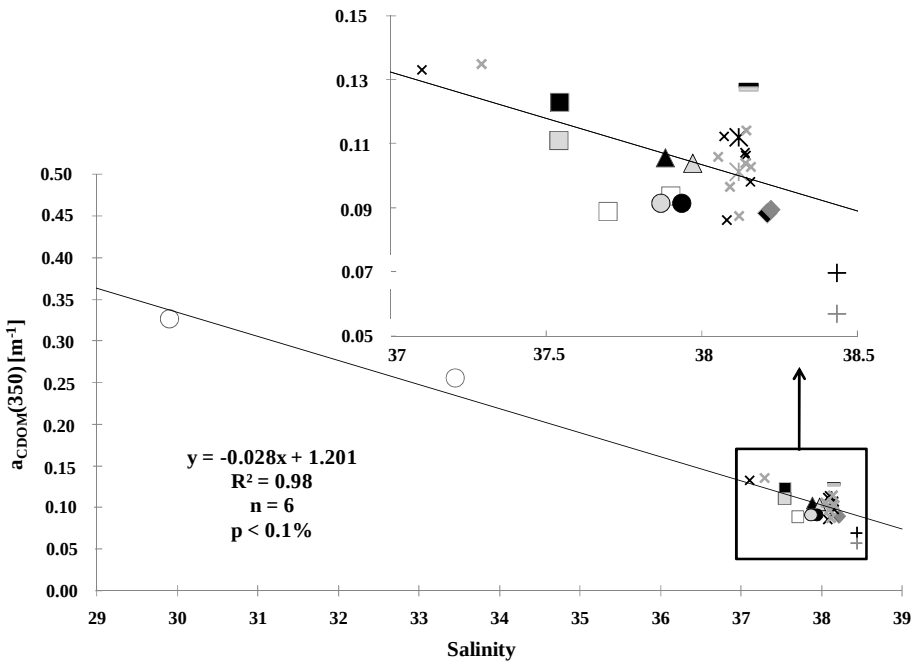

Fig. 3. Relationship between salinity and CDOM absorption at 350 nm (in m^{-1}) acquired at SOFCOM station at 2 m (black mark, n=13) and 5 m (gray mark, n=14) depths. All data in Table 2 for a_{CDOM}(350 nm) are included. Each mark corresponds to a sampling date: crosses for the period 7 November 2007–29 April 2008; triangle for 9 June 2008; square for 23 June 2008; circle for 10 July 2008; plus for 23 September 2008; diamond for 14 October 2008; dash for 25 November 2008 and star for 4 December 2008. Data from Rhône plume acquired in May 2008 during CHACCRA cruise at 2 m (white circle, n=2) and 5 m (white square, n=2) were also plotted. The mixing line was established using SOFCOM data at 2 m depth with salinity <38 (6 May 2008; 9 June 2008; 23 June 2008; 10 July 2008) plus Rhône estuary stations (CHACCRA cruise data) at 2 m depth as well (n=2).

BGD
7, 5675–5718, 2010

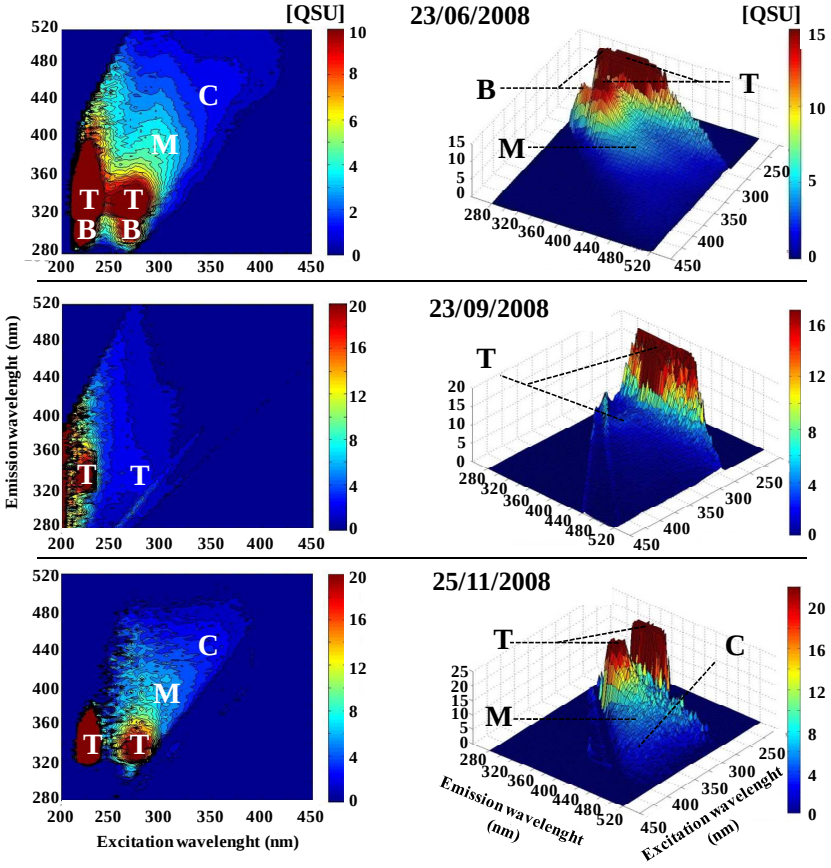

Fig. 4. 2-D (left panel) and 3-D (right panel) EEM contour plots of CDOM (in QSU) acquired at SOFCOM station at 2 m depth on 23 June 2008, 23 September 2008 and 25 November 2008. These spectra illustrated the fluorophore peak positions observed during this study. 3-D spectra are shown from reverse side to facilitate viewing of humic-like peak (peak C).

BGD
7, 5675–5718, 2010

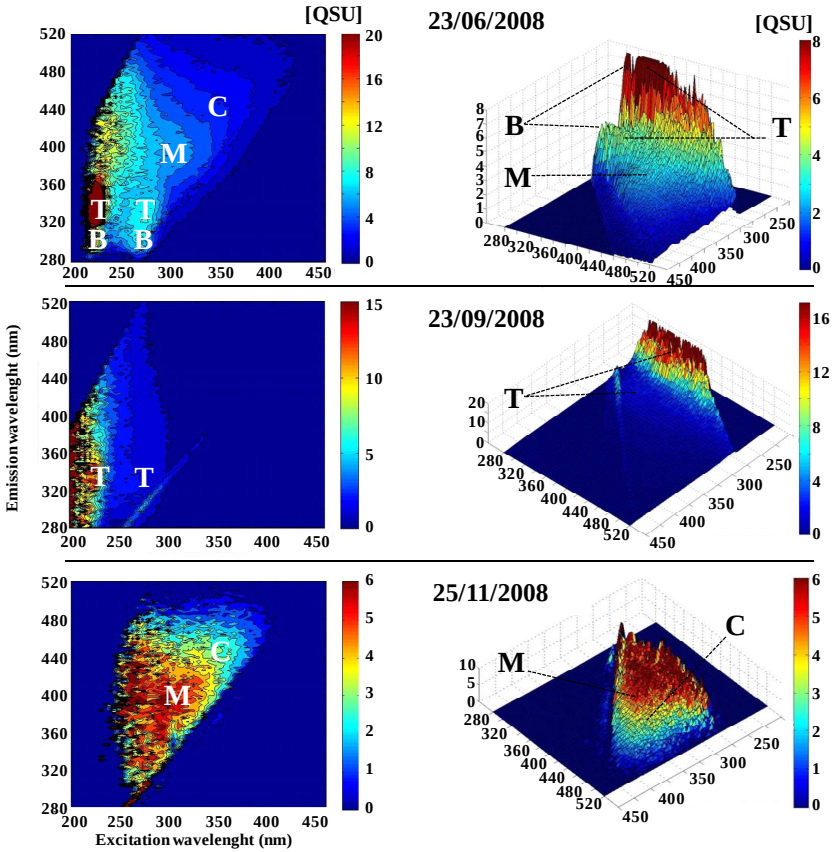

Fig. 5. 2-D (left panel) and 3-D (right panel) EEM contour plots of CDOM (in QSU) acquired at SOFCOM station at 5 m depth on 23 June 2008, 23 September 2008 and 25 November 2008. These spectra illustrated the fluorophore peak positions observed during this study. 3-D spectra are shown from reverse side to facilitate viewing of humic-like peak (peak C).

BGD
7, 5675–5718, 2010

Surface CDOM optical properties in the Bay of Marseilles

J. Para et al.

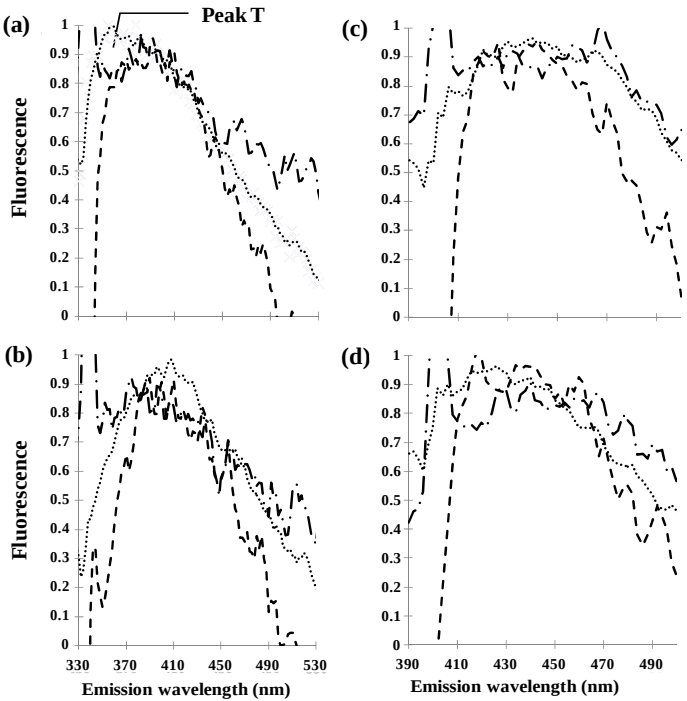

Fig. 6. Emission fluorescence spectra of peak M **(a** and **b**) at Ex(λ)=300 nm and peak C (**c** and **d**) at Ex(λ)=350 nm acquired on 23 June 2008 (dotted line), 23 September 2008 (dotted dashed line) and 25 November 2008 (dashed line) at 2 m (upper panel) and 5 m (bottom panel) depths. These emission spectra were normalized to the maximum emission intensity in the range 380–400 nm for the peak M and 430–450 nm for the peak C. These spectra were smoothed by a moving average order 3 which imposes a red shifted of 5 nm.

BGD
7, 5675–5718, 2010

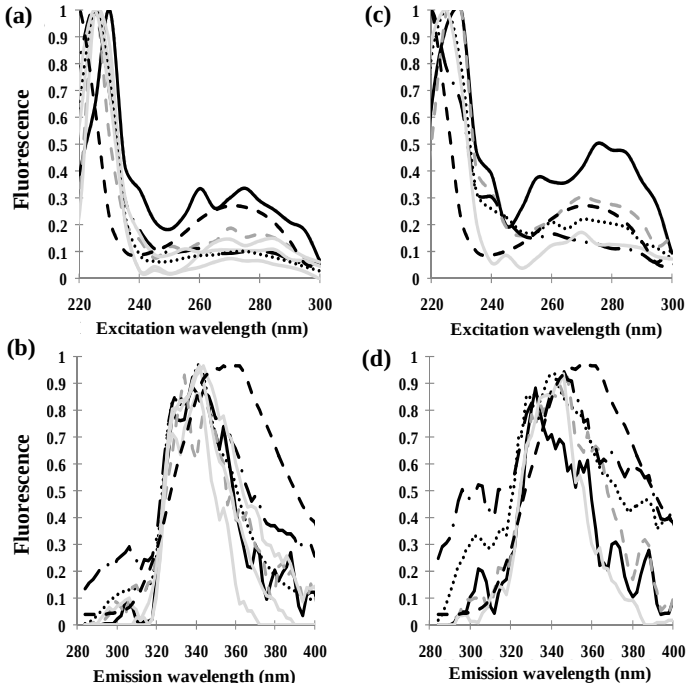

Fig. 7. Fluorescence spectra of peak T at both depths acquired on 9 June 2008 (dark solid line), 23 June 2008 (black dotted line), 10 July 2008 (grey dashed line), 23 September 2008 (black dashed-dotted line) and at others dates (grey solid line) reported in Table 3. All these spectra are compared to a solution standard at 75 µg l^{-1} of free dissolved L-tryptophan (>98%, Sigma-Aldrich, black dashed line). (**a** and **c**) excitation spectra with Em=340 nm at 2 and 5 m depth, respectively, normalized to the maximum value intensity in the 220–240 nm range. (**b** and **d**) emission spectra with Ex=230 nm at 2 and 5 m depth, respectively, normalized to the maximum value intensity in the 320–360 nm range. In order to reduce noise, all these emission-excitation spectra were smoothed by a moving average order 3 which imposes a red shifted of 5 nm.

BGD
7, 5675–5718, 2010

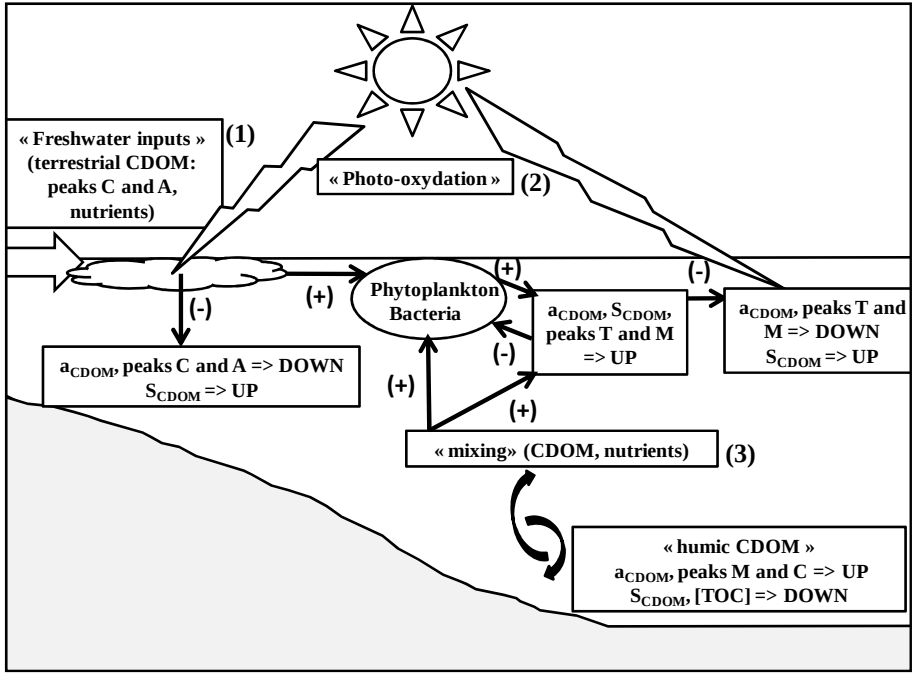

Fig. 8. Synthesis of processes (Rhône River plume intrusion (1), photo-oxydation of CDOM (2) and deep water mixing (3)) that drive surface CDOM dynamic and content in the Bay of Marseilles and their direct and indirect effects (positive or negative) on CDOM optical properties.

BGD
7, 5675–5718, 2010